# Insulin Is Transcribed and Translated in Mammalian Taste Bud Cells

Máire E. Doyle,[1] Jennifer L. Fiori,[1] Isabel Gonzalez Mariscal,[1] Qing-Rong Liu,[1] Erin Goodstein,[1] Hyekyung Yang,[1] Yu-Kyong Shin,[1] Sara Santa-Cruz Calvo,[1] Fred E. Indig,[2] and Josephine M. Egan[1]

[1]Laboratory of Clinical Investigation/Diabetes Section, National Institute on Aging, National Institutes of Health, Baltimore, Maryland 21224; and [2]The Confocal Imaging Facility, National Institute on Aging, National Institutes of Health, Baltimore, Maryland 21224

We and others have reported that taste cells in taste buds express many peptides in common with cells in the gut and islets of Langerhans in the pancreas. Islets and taste bud cells express the hormones glucagon and ghrelin, the same ATP-sensitive potassium channel responsible for depolarizing the insulin-secreting $\beta$ cell during glucose-induced insulin secretion, as well as the propeptide-processing enzymes PC1/3 and PC2. Given the common expression of functionally specific proteins in taste buds and islets, it is surprising that no one has investigated whether insulin is synthesized in taste bud cells. Using immunofluorescence, we demonstrated the presence of insulin in mouse, rat, and human taste bud cells. By detecting the postprocessing insulin molecule C-peptide and green fluorescence protein (GFP) in taste cells of both insulin 1-GFP and insulin 2-GFP mice and the presence of the mouse insulin transcript by *in situ* hybridization, we further proved that insulin is synthesized in individual taste buds and not taken up from the parenchyma. In addition to our cytology data, we measured the level of insulin transcript by quantitative RT-PCR in the anterior and posterior lingual epithelia. These analyses showed that insulin is translated in the circumvallate and foliate papillae in the posterior, but only insulin transcript was detected in the anterior fungiform papillae of the rodent tongue. Thus, some taste cells are insulin-synthesizing cells generated from a continually replenished source of precursor cells in the adult mammalian lingual epithelium. (***Endocrinology*** **159: 3331–3339, 2018)**



There are many similarities between islets of Langerhans and taste bud cells (TBCs) of the tongue, both in terms of architecture and peptide hormone expression. They are both discrete organs of epithelial origin that function differently from their surrounding tissue and possess their own microvasculature. TBCs express many gut and islet hormones and their cognate receptors (1). For example, we and others have reported that proglucagon and proghrelin products normally found in islets of Langerhans and enteroendocrine cells are also synthesized in TBCs of mice, rats, and monkeys (2, 3). Islets and TBCs both express the proconvertases PC1/3 and PC2 (3), enzymes necessary for generating active peptides from their precursors. Conversely, islet cells express prototypic taste receptors and their downstream signaling molecules (2). However, islets and taste buds serve different purposes in the regulation of nutrient ingestion and processing (1). Islet hormone secretion maintains homeostasis in the availability of energy for physiological processes and is primarily regulated by the postabsorptive products of food consumption (4, 5). In contrast, hormones secreted from TBCs in response to nutrient entry into the oral cavity modify the intensity of the signaling from tastants and act as integrators of information from the various components in food (*i.e.*, preabsorptive effects of food components) (1, 6).

Because of the harsh nature of their environment, TBCs have a limited life span and must undergo continuous replacement every 8 to 12 days throughout life (6, 7). The lingual epithelium in the intragemmal regions of the tongue is the source of progenitor cells for TBCs.

ISSN Online 1945-7170

Received 31 May 2018. Accepted 19 July 2018.
First Published Online 27 July 2018

Abbreviations: AS, Airyscan; EdU, 5-ethynyl-2′-deoxyuridine; GFP, green fluorescence protein; HBSS, Hanks Balanced Salt Solution; ISH, *in situ* hybridization; NDRI, National Disease Research Interchange; NIA, National Institute on Aging; NIH, National Institutes of Health; NOD, nonobese diabetic; TBC, taste bud cell; TBS, Tris-buffered saline.

Once these progenitor cells have committed to becoming TBCs, they migrate to the perigemmal regions of the taste bud, where they express LGR5 (formerly known as GPR49) (8). Lineage tracing demonstrates that all mature TBCs are derived from precursor cells in the intragemmal spaces at the base of the taste bud (6, 9, 10). The regular replenishment of adult TBCs is in sharp contrast to adult islet cells, which do not have a stem cell pool (11).

Building on our previous body of work in pancreas and taste buds (12), we used standard immunohistochemical methods to investigate whether insulin is present in TBCs and then verified the synthesis and processing of insulin gene products using several independent methods. We probed for insulin expression in the three types of taste papillae found in mammalian tongues, namely the posterior circumvallate and foliate and the anterior fungiform papillae. We further investigated which of the three types of terminally differentiated TBCs present in taste buds—type I (salt-tasting), type II (sweet-, bitter-, and umami-tasting), and type III (sour-sensing)—express insulin.

## Material and Methods

### Ethics statement

All animals were cared for and studied in accordance with guidelines of the US Public Health Service Policy on the Humane Care and Use of Laboratory Animals and the National Institutes of Health (NIH) Guide for the Care and Use of Laboratory Animals. The vivarium located at the Biomedical Research Center is fully accredited by the American Association for Accreditation of Laboratory Animal Care, and all procedures were approved by the Animal Care and Use Committee of the National Institute on Aging (NIA) Intramural Program. Human lingual tissue was procured from a cadaver for the NIA by the National Disease Research Interchange (NDRI; Philadelphia, PA). The procurement of lingual cadaveric tissue by the NDRI for research proposes was reviewed by the Office of Human Subjects Research/NIH and was deemed to be institutional review board exempt (no. 12706).

### Rodents

Adult male C57/BL6 mice, female nonobese diabetic (NOD) Shi/LtJ mice, and breeding pairs of Insulin-1-GFP [B6.Cg-Tg(Ins1-EGFP)1Hara/J (13)] and Insulin-2-GFP [C57BL/6-Tg(Ins2-luc/EGFP/Tk)300Kauf/J (14)] mice were purchased from The Jackson Laboratory (Bar Harbor, ME). Adult male Long-Evans and Sprague-Dawley rats (Charles River Laboratories, Germantown, MD) were singly housed in standard cages. Sprague-Dawley rats developed diabetes by consumption of a high-fat, high-sugar diet. All rodents were kept in a climate-controlled vivarium maintained on a 12-hour light: 12-hour dark cycle. Food and water were available *ad libitum*.

### Immunofluorescence staining of human, rat, and mouse tissues

Rat and mouse tongues were fixed in 10% neutral-buffered formalin (Thermo Fisher Scientific, Waltham, MA) and then cryoprotected with 20% sucrose (Sigma-Aldrich, St. Louis, MO) in 0.1 M phosphate buffer (Quality Biologicals, Gaithersburg, MD) overnight at 4°C. Human tongues were placed in 10% neutral buffered formalin within 12 hours of death by the NDRI procurement team and shipped in formalin. Upon arrival at the NIA/NIH, the lingual epithelium was removed and processed in the same manner as the rodent tissues. Tissue sections (8- to 12-μm thickness) were cut using a Leica CM1950 cryostat (Leica Biosystems, Buffalo Grove, IL) and mounted onto Superfrost Plus Micro slides (VWR, Radnor, PA) and stored at −20°C until used for immunostaining. To study the fungiform papillae, serial sections (12 μm) from the anterior portion of the mouse and rat tongue were cut in the manner of Gaillard *et al.* (15). To permeabilize the cells in the tissue, slides were placed in Tris-buffered saline (TBS) (pH, 7.4; Quality Biologicals) with 0.2% Triton-X 100 (Sigma-Aldrich) for 5 minutes at room temperature. They were then washed three times (2 minutes) in TBS. Antigen retrieval was performed by placing the slides in 10 mM of sodium citrate buffer (pH, 6.0; Vector Laboratories, Burlingame, CA) at 95°C for 30 minutes. The slides were allowed to cool at room temperature in the citrate buffer for a further 30 minutes and were then rinsed in TBS as before.

Sections were incubated with normal goat serum block consisting of 2% goat serum, 1% OmniPur® BSA Fraction V (Sigma-Aldrich), 0.1% gelatin, (Sigma-Aldrich), 0.1% Triton X-100 (Sigma-Aldrich), 0.05% Tween 20 (Sigma-Aldrich), and 0.05% sodium azide (Sigma-Aldrich) in TBS for 1 hour at room temperature. Sections were then incubated in primary antibody diluted in the same normal goat serum block. The following primary antibodies were used: rabbit anti–C-peptide (1:100) used only in the rat taste papillae, from Cell Signaling Technology (Danvers, MA) (16); guinea-pig anti–C-peptide (1:100) used only in mouse taste papillae, from Abcam (Cambridge, MA) (17); rat anti-cytokeratin 8 (1:100) from Developmental Studies Hybridoma Bank (University of Iowa, Iowa City, IA) (18); rabbit anti-cytokeratin 8 (1:100) from Abcam (19); rabbit anti-GFP (1:50) from Santa Cruz Biotechnology (Dallas, TX) (20); mouse anti-insulin (1:50) used in rat and human taste papillae from Sigma Aldrich (21); guinea pig anti-insulin (1:100) used in the mouse tissue, from Millipore-Sigma (Burlington, MA) (22); mouse anti-Ki67 (1:50) from DAKO–Agilent Technologies (Santa Clara, CA) (23); rabbit anti-Lgr5 (1:50) from Abcam (24); rabbit anti-NTPDase2 (1:100) from J. Sévigny (Université Laval, Québec City, QC, Canada) (25); rabbit anti-PLC$\beta$2 (1:200) from Santa Cruz Biotechnology (26); and rabbit anti-SNAP25 (1:200) from Sigma Aldrich (27). Sections were then washed three times (2 minutes) in 0.1% Tween-20 in 1× TBS (pH, 7.4), followed by incubation with the specific secondary antibody diluted in the normal goat serum block for 1 hour at room temperature. Secondary antibodies used were goat anti-rabbit IgG (H+L) Alexa Fluor 568 (28); goat anti-mouse IgG (H+L) Alexa Fluor 647 (29); goat anti-guinea pig IgG (H+L) Alexa Fluor 488 (30); and goat anti-mouse IgG (H+L) Alexa Fluor488 (31), all from Thermo Fisher Scientific, and goat anti-rat Cy3 from Jackson Immunoresearch Laboratories (West Grove, PA) (32). After washing in 0.1% Tween-20 in 1× TBS as before, sections were incubated for 15 minutes with 4′,6-diamidino-2-phenylindole (Sigma Aldrich) for nuclear staining. Slides were next washed in TBS twice for 2 minutes each time before being mounted with Permafluor Mountant (Thermo Fisher Scientific).

Controls used were incubation without primary antibody (Supplemental Fig. 1A); incubation with rabbit (Vector Laboratories), rat (US Biological Life Sciences, Salem, MA), and guinea pig serum (US Biological Life Sciences) (Supplemental Fig. 1B); and preabsorption of the insulin antibodies (Supplemental Fig. 1C). All control sera concentrations were within a sevenfold range of the concentration of all antibodies. Preabsorption with 10-fold excess of the immunogen was done with human insulin in the case of the guinea pig anti-insulin and mouse anti-insulin antibodies. Appropriate no-primary-antibody controls were prepared with each individual batch of slides.

Airyscan (AS) imaging was performed on the same LSM 880 used for confocal imaging, using the same Plan Apochromat 63×/NA 1.4 or 40×/NA 1.3 objectives as used with confocal. Regular AS mode has a pixel resolution of 0.04 μm XY and 0.2 μm Z. We used the default Zen AS setting for three-dimensional imaging and processing by Zen of the raw AS image (AS-SR mode). Brightness and contrast were adjusted with Zen similar to all AS images.

## RNAscope *in situ* hybridization

RNAscope *in situ* hybridization (ISH) probes were customer designed by Advanced Cell Diagnostics Inc. (Hayward, CA) for mouse Ins2 (10 ZZ pairs targeting 2-470 of NM_008387.5) in C1 (Mm-Ins2-O1) and C2 (Mm-Ins2-O1-C2) channels. Catalog RNAscope ISH probes Plcb2 (20 ZZ pairs targeting 2-971 of NM_177568.2) in C2 (Mm-Plcb2-C2) channel and Ncam1 (20 ZZ pairs targeting 5397-6437 of NM_001113204.1) in C1 (Mm-Ncam1-O1) channel were ordered from Advanced Cell Diagnostics Inc. Mouse tongues were extracted, processed, and frozen as described previously and stored at −80°C. Mouse pancreas was removed within 2 minutes of death from the abdominal cavity and frozen in 100 mL of −50°C isopentane, placed in liquid nitrogen, and stored at −80°C in a sealed bag. The cryostat sectioning, fixation, protease pretreatment, probe hybridization, preamplification, amplification, and fluorescent labeling steps were performed as described in the manufacturer's protocol (33, 34), with the exception that pancreas sections were treated with protease IV for 10 minutes instead of the 30 minutes at room temperature used for the tongue sections. The negative control used for the ISH was a universal control probe targeting the *dapB* gene (accession no.EF191515) from the *Bacillus subtilis* strain, and the positive controls were probes targeting *Ubc* (ubiquitin C), *Pp1b* (cyclophilin B), and Polr2A (DNA-directed RNA polymerase II subunit RPB1).

## Image acquisition and analysis

Confocal fluorescence images were captured using Zen software under either a 20×, 40× oil, or 63× oil objective on either a Carl Zeiss LSM-880 or LSM-710 confocal microscope (Jena, Germany). Apart from the images of the mouse/rat foliate and fungiform papillae, all images are of sections from the circumvallate papillae from mouse, rat, and human tongues. Acquisition parameters (*e.g.*, pinhole size, gain, offset) were set using the range indicator mode of Zen and are within the following range of intensity: 0-65536 (16 bit), 0-4096K (12 bit), and 0-512 K (8 bit). Threshold settings for detecting true signal in slides processed through primary and secondary antibody staining were set using the no primary antibody controls (Supplemental Fig. 1A). Appropriate no-primary-antibody controls were prepared with each individual batch of slides. All no-primary-antibody, serum (Supplemental Fig. 1B), and preabsorption controls (Supplemental Fig. 1C) were captured using the same settings (*e.g.*, range, offset) that were used to capture actual staining from slides treated with both primary and secondary antibodies prepared at the same time. Confocal images were rendered for publication purposes using Canvas 12 software (Canvas GFX Inc., Fort Lauderdale, FL), and brightness (+80) and contrast (+23) were adjusted to the same degree for each of the figures shown in this manuscript. The color coding for the scale bars in the confocal images is as follows: red is 10 μm, white is 20 μm, and yellow is 50 μm.

## 5-Ethynyl-2′-deoxyuridine labeling and detection

5-Ethynyl-2′-deoxyuridine (EdU; Thermo Fisher Scientific) was injected 5 days before euthanasia of C57Bl6J mice to ensure its ultimate incorporation into the DNA of differentiated TBCs. Tongues were fixed, processed, and frozen as described previously, and sections were cut at 10-μm thickness. Sections were treated with antigen retrieval with citrate buffer as previously described, then permeabilized with 0.5% Triton X-100 in TBS followed by incubation in Click-iT solution for detection of EdU using Alexa Fluor 594, which was prepared according to the manufacturer's instructions (Thermo Fisher Scientific). Slides were washed in 3% BSA in TBS, and then immunostaining for insulin and imaging was performed as described previously.

## Isolation of mouse lingual epithelium

The dorsal epithelium of mouse tongue containing both anterior and posterior taste buds was isolated using modifications of a previously reported method by Luo *et al.* (35). Mouse tongues were washed with PBS (Thermo Fisher Scientific) and placed into Hanks Balanced Salt Solution (HBSS; Thermo Fisher Scientific). An enzyme cocktail (1 mL) containing 1 mg/mL of collagenase A (Roche Applied Science; Indianapolis, IN), 2.5 mg/mL of dispase II (Roche Applied Science), and 1 mg/mL of trypsin inhibitor I-S (Sigma-Aldrich) in HBSS was injected uniformly under the epithelium of the dissected tongue. After incubation for 20 to 30 minutes in HBSS at room temperature, the tongue was placed into an EGTA-containing solution (2 mM EGTA, 139 mM NaCl, 5 mM KCl, 10 mM Hepes, 10 mM glucose, 10 mM sodium pyruvate, and 5 mM sodium bicarbonate, pH 7.2) for 10 minutes at room temperature. The epithelium was then gently peeled from the underlying muscle layer under a dissecting microscope (Carl Zeiss) and placed in HBSS. Mouse lingual epithelium was then used for extraction of mRNA and insulin ELISA as described later.

## Insulin extraction and ELISA

The basal epithelial layer of the mouse tongue was isolated as described previously (35). Insulin was extracted from 20 mouse lingual epithelia (anterior and posterior) and an equivalent weight of tissue of mouse skeletal muscle (quadriceps) and tongue muscle by placing them in acid ethanol (0.18 M of HCl in 70:30 v/v ethanol:HCl), and the tubes were put in a sonicating bath overnight at 4°C. The tube containing the tissue was left at 4°C with continuous agitation for 12 hours. The acid ethanol was then neutralized with an equimolar equivalent of sodium hydroxide and lyophilized to dryness. The remaining solid was dissolved in water. Mouse insulin extracted from the lingual epithelium and muscle was measured by an

enzyme-linked immunosorbent assay kit from Crystal Chem Inc. (Downers Grove, IL), an assay that has been used regularly in our laboratory (36, 37).

### RNA isolation, reverse transcription, and quantitative RT-PCR

Mouse lingual epithelium was cut into two parts anterior to the lingual prominence and lysed in Trizol (Thermo Fisher Scientific) using the Omni International (Kennesaw, GA) Bead Ruptor 24 using RNAase/DNASe free, 1.4 mm, ceramic beads for a total of 55 seconds at room temperature. Mouse total RNAs were then extracted from the anterior (fungiform taste papillae) and posterior (circumvallate and foliate) portions of the lingual epithelium separately using the Trizol protocol (Thermo Fisher Scientific). Single-strand cDNA was synthesized from total RNA using the iScript cDNA Synthesis kit (Bio-Rad, Hercules, CA). For RNA reverse transcription quantitative real-time PCR assays, the fluorescent FAM-labeled and minor groove binder-conjugated TaqMan probes of mouse Ins1 (Mm01950294_s1) and Ins2 (Mm00731595_gH) TaqMan probes and the fluorescent VIC-labeled endogenous control Actin probe (catalog no. 4351315; Applied Biosystems, Foster City, CA) were used for duplex TaqMan assay with technical replicates. ABI 7900HT Sequence Detection System (Thermo Fisher Scientific) default program was used for RT-PCR with 40 cycles. The relative fold change is calculated using the formula: $2^{-\Delta\Delta CT}$ formula. GraphPad (La Jolla, CA) Prism 6.0 software was used for statistical analysis, and data are presented as means ± SEM.

## Results

### Rodent and human circumvallate and foliate TBCs express insulin

Using standard immunohistochemical methods, we found that adult mouse and rat TBCs in circumvallate and foliate papillae express insulin (Fig. 1A and 1B). We also found insulin immunoreactivity in human TBCs in the circumvallate papilla (Fig. 1C). We did not find any insulin immunoreactivity in the fungiform papillae of rat or mouse tongues (Fig. 1A and 1B); we examined 100 mouse and 20 rat fungiform papillae. When antibodies specific for the type I, II, or III TBCs [NTPDase (38), PLC$\beta$2 (39), and SNAP25 (40), respectively] were used and costaining for insulin in TBCs of the circumvallate papillae was performed, it appears that there was costaining with insulin and both type II and type III markers (Fig. 2). To gain a clearer perspective of the subset of TBCs that express insulin, we performed ISH for type II and type III cell markers, namely PLC$\beta$2 and NCAM (Fig. 3A) in the taste buds of the circumvallate papillae. We found insulin in TBCs that have the PLC$\beta$2 transcript but not in the nuclei of cells positive for the NCAM transcript. Of note, not every PLC$\beta$2-expressing nucleus had insulin. For comparison, we included ISH for insulin performed on the mouse pancreas (Fig. 3B).

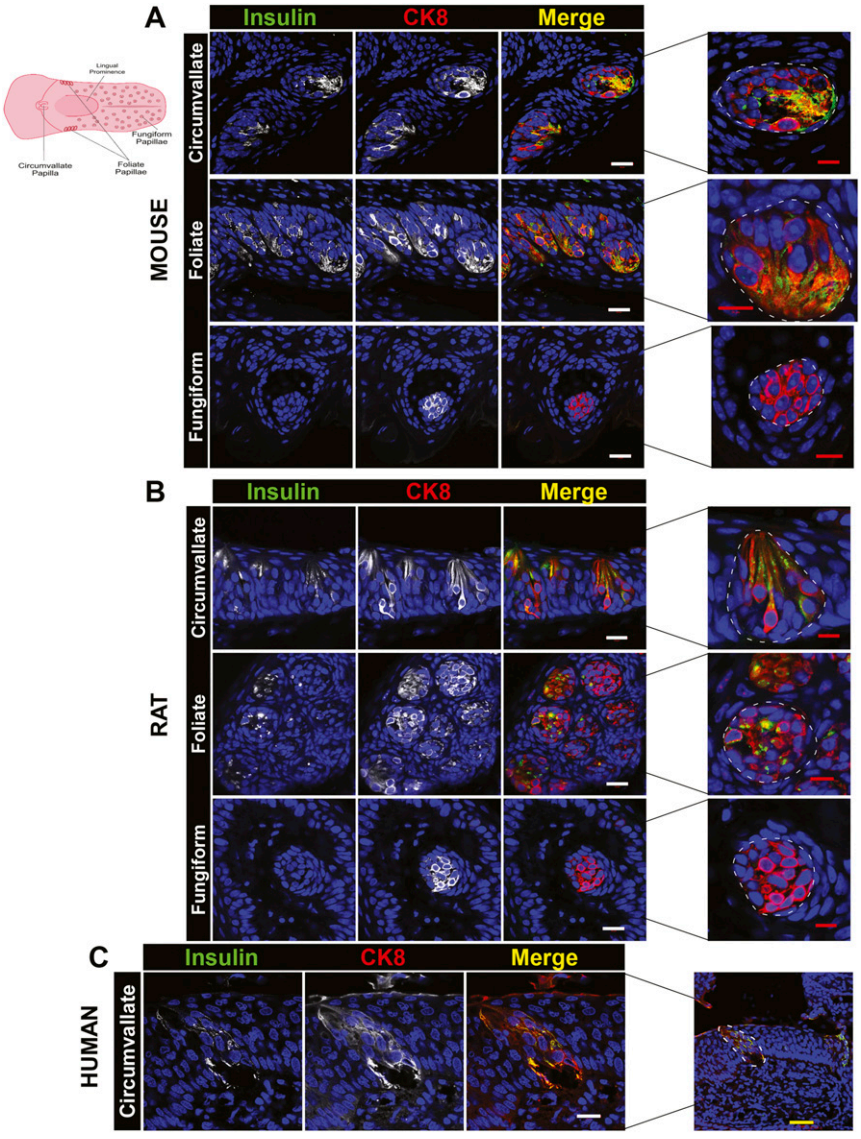


**Figure 1.** Insulin immunoreactivity is found in TBCs of rodent circumvallate and foliate papillae and in the circumvallate papillae of the human tongue. Immunofluorescence staining of (A) C57BL6 mouse and (B) Long-Evans rat lingual tissue for insulin and cytokeratin 8 (CK8), a marker of mature taste cells, is shown. Note the characteristic granular nature of the insulin immunoreactivity compared with the filamentous staining of CK8. (C) Insulin is expressed in several TBCs in an individual taste bud in human circumvallate papillae. CK8 costaining in a human taste bud in a section taken from human cadaveric tongue, male aged 76 years, was procured by the NDRI. Insert shows the location of the taste papillae in the mouse tongue. Positive and negative controls are shown in Supplemental Fig. 1. Scale bars: red is 10 μm, white is 20 μm, and yellow is 50 μm.

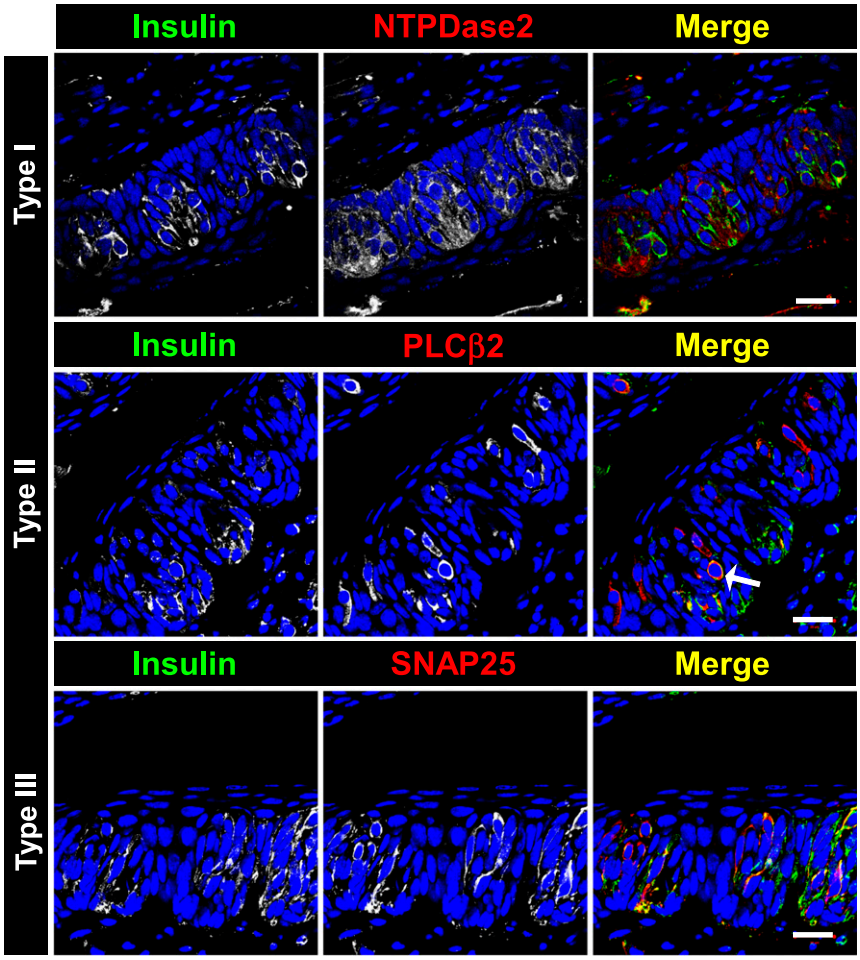


**Figure 2.** Insulin appears to be expressed in a subset of TBCs. Previously verified (15) antibodies to NTPDase2, PLC$\beta$2, and SNAP25 were used to label type I, II, and III cells, respectively, in mouse circumvallate papillae. Insulin seems to be coexpressed with PLC$\beta$2 and SNAP25, as indicated by the white arrow. Scale bar, 20 $\mu$m.

## Insulin transcript levels are higher in the anterior (fungiform papillae) portion of the mouse tongue

We looked for an insulin transcript signal in the lingual epithelium using both ISH performed on frozen sections of the foliate and fungiform papillae and RT-PCR on RNA extracted from either the anterior (fungiform papillae) or posterior (foliate and circumvallate) portions of the epithelium of the tongue. We found that the insulin transcript was expressed in every single TBC that expressed PLC$\beta$2 in both the foliate and fungiform papillae (Fig. 4A). The insulin 2 gene is more highly expressed than the insulin 1 gene throughout the lingual epithelium (Fig. 4B). Note that the level of insulin 1 and insulin 2 mRNA is higher in the anterior portion containing the fungiform papillae than in the posterior portion containing both the foliate and circumvallate papillae.

## Insulin is synthesized and processed in mammalian TBCs

Proinsulin is processed to mature immunoreactive insulin in $\beta$ cells in the islet of Langerhans. C-peptide is an inactive byproduct of proinsulin cleavage, and its presence indicates that proinsulin is processed into mature insulin. As a consequence of the processing, C-peptide should be present in every cell that also has produced insulin. As in $\beta$ cells, C-peptide and insulin are always coexpressed in TBCs: They are never found in isolation (Fig. 5A). We also showed that C-peptide is present in TBCs of mouse circumvallate papillae (Fig. 5B).

Rodents have two nonallelic insulin genes; the Ins2 gene is an ortholog to insulin genes in other mammals, and the Ins1 gene is a paralog originating from a reverse-transcribed, partially processed mRNA of the Ins2 gene (41, 42). To use another method to demonstrate that insulin is expressed in taste cells, we looked for the presence of green fluorescent protein (GFP) in the tongues of both Insulin-1-GFP (13) and Insulin-2-GFP (14) mice that express GFP under the control of the mouse Ins1 and Ins2 promoters, respectively. TBCs in both mice were found to be positive for GFP (Fig. 5C). We did not observe GFP expression in the extragemmal spaces of the lingual epithelium of the GFP-expressing mice or in TBCs of C57BL6 mice that do not express GFP (Fig. 5C; rightmost panel). As expected, we observed GFP in the islets of frozen sections of pancreas taken from both strains of mice but not in nonislet pancreatic tissue (Fig. 5D). These data prove definitively that both mouse insulin genes are expressed in TBCs, and only in TBCs, within taste buds.

## Insulin-containing TBCs are generated from highly proliferative progenitor cells in the lingual epithelium

All three types of mature TBCs are terminally differentiated, do not proliferate, and must be continually renewed from progenitor cells in the intragemmal spaces every 8 to 12 days (6, 7). Migration of these undifferentiated cells in mice from the base of the taste bud (in the circumvallate taste papillae) occurs within 1 day of replication as marked by the incorporation of the thymidine analogue EdU (7). By progressively monitoring the EdU-labeled cells, Perea-Martinez *et al.* (7)

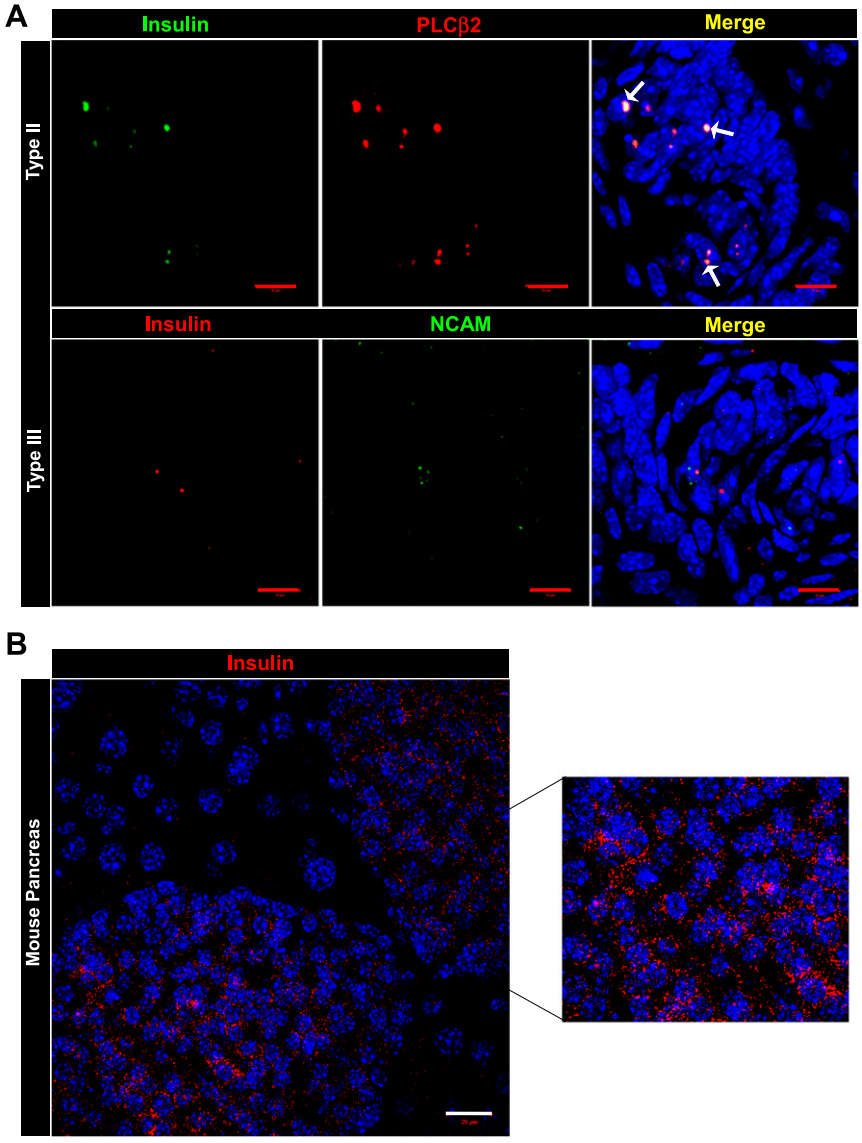


**Figure 3.** Insulin mRNA is found only in type II cells in the mouse circumvallate papilla. (A) Using probes to the transcripts of PLC$\beta$2 and NCAM, which are found in type II and type III cells, respectively, we showed that insulin colocalizes only with PLC$\beta$2 in the circumvallate papillae in the mouse tongue (white arrows). (B) ISH for insulin in the islets of a mouse pancreas. Scale bars: red is 10 $\mu$m, and white is 20 $\mu$m.

demonstrated that most reach the mucosal side of the taste bud within 5 days of initial EdU administration. By replicating this EdU Click-iT chemistry detection method and immunostaining for insulin, we showed that cells had proliferated within the last 5 days and progressed into the taste bud to become mature TBCs that express insulin (Fig. 6A). The presence of these highly proliferative precursor cells in the human tongue at age 70 years is demonstrated by the extent of Ki67 immunoreactivity in humans (Fig. 6B). By staining for the specific taste progenitor cell marker Lgr5 in circumvallate papillae (8), we demonstrated that there are abundant proliferating progenitor cells in the older human tongue (Fig. 6B).

### Insulin is expressed in TBCS of diabetic rodents

Insulin synthesis and processing also occurred in TBCs in mouse models of both major forms of diabetes. Insulin was readily apparent in TBCs of the NOD Shi/LtJ mouse, a model of autoimmune diabetes (type 1 diabetes) (Fig. 6C). The mouse exhibited classic signs of diabetes [*i.e.*, elevated fasting blood glucose levels (>240 mg/dL) and islet infiltration] at the time of euthanasia. Moreover, TBCs in a diabetic Sprague-Dawley rat fed a high-fat/high-sugar diet, a model of type 2 diabetes (fasting blood glucose level ~275 mg/dL) also displayed robust, readily apparent insulin immunoreactivity (Fig. 6D). We did not observe any differences in intensity levels of fluorescence from the insulin signal in circumvallate papillae between the normoglycemic and diabetic models (data not shown).

### Quantification of extracted lingual insulin by ELISA

To confirm that insulin is indeed fully processed in lingual tissue, we used the established method of acid-ethanol extraction (43) to extract insulin from mouse lingual epithelium and measured the total amount of insulin using an ELISA. However, we had to combine epithelia from up to 20 mice to get 0.1 nmol of mouse insulin in total. An equivalent weight of mouse pancreas had 10 times more insulin than that measured in the lingual epithelium. No insulin was detected in similarly treated tissue of equivalent weight from either mouse skeletal or lingual muscle.

## Discussion

To establish that insulin immunostaining was not islet-derived insulin that was endocytosed by the cells, we used several technical methods to demonstrate insulin synthesis and processing in TBCs. Preproinsulin is synthesized in the endoplasmic reticulum, where the preportion is then removed enzymatically. Proinsulin is next converted there by the prohormone-converting endopeptidases PC3 (also known as PC1) and PC2 and the exoprotease carboxypeptidase H into mature insulin and

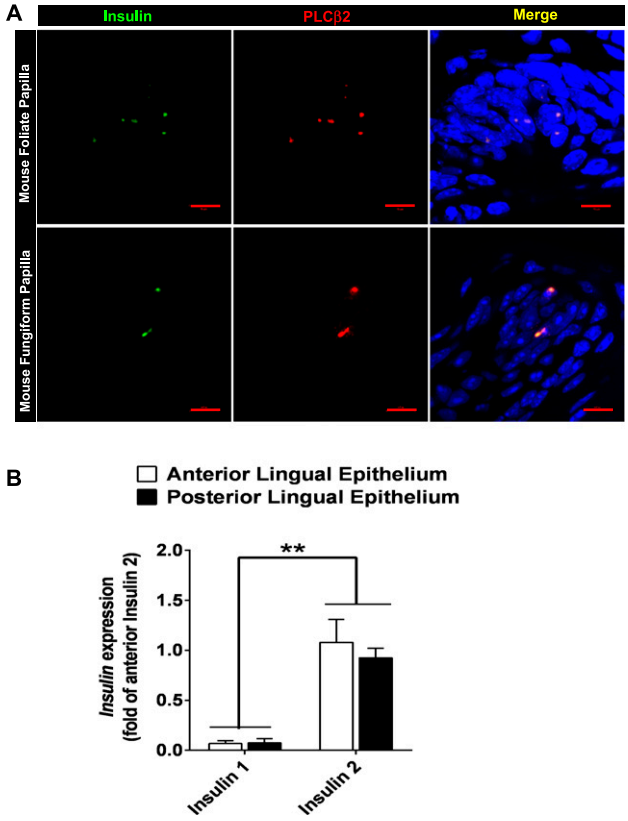


**Figure 4.** Insulin transcript is present in the foliate and fungiform papillae of the mouse tongue. (A) Insulin transcript was detected by ISH and was found to colocalize with PLC$\beta$2 transcript in both the foliate and fungiform papillae of mice. Note that in the fungiform and foliate papillae, there appears to be complete overlap between insulin and PLC$\beta$2 transcripts. Scale bar, 10 $\mu$m. (B) Quantitative RT-PCR data showing the levels of insulin 1 and insulin 2 transcripts (normalized to mouse $\beta$-actin – internal control) and shown relative to the levels of insulin 2 in the anterior lingual epithelium (Error bars, mean $\pm$ SEM; n = 4 per condition). $^{**}P < 0.005$.

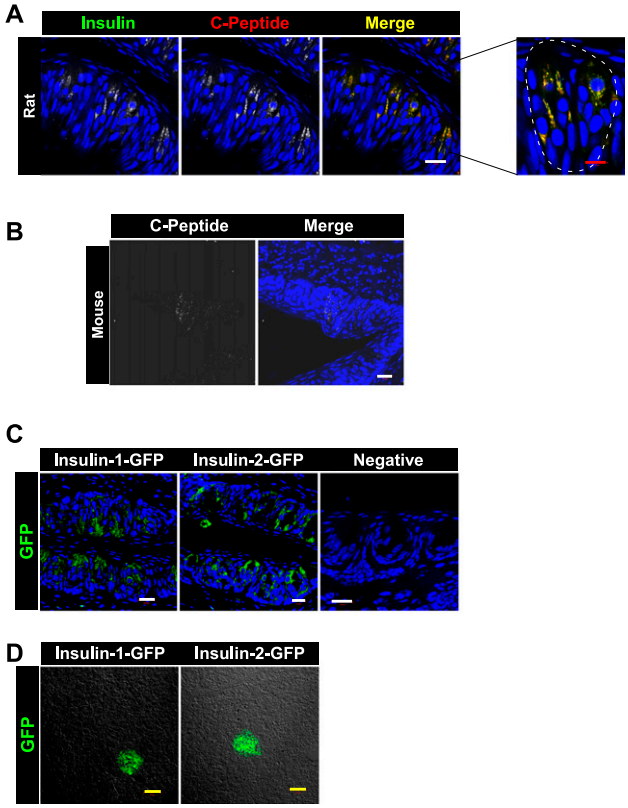


**Figure 5.** Rodent TBCs synthesize insulin. (A) Rat TBCs are shown coexpressing the insulin gene products insulin and C-peptide. (B) Mouse TBCs are shown expressing C-peptide as well. (C) Mice expressing GFP under the control of either the insulin 1 promoter (Insulin-1-GFP mice) or the Ins2 promoter (Insulin-2-GFP mice) had GFP immunoreactivity in their TBCs. No GFP immunoreactivity was found in TBCs of C57BL6 mice. (D) Green fluorescence is evident in islets of Langerhans of Insulin-1-GFP and Insulin-2-GFP mice. Scale bars: red is 10 $\mu$m, white is 20 $\mu$m, and yellow is 50 $\mu$m.

the inactive byproduct C-peptide. Therefore, the presence of both insulin and C-peptide is considered the *conditio sine qua non* for active synthesis of insulin in a cell (44). We showed that C-peptide is indeed present by immunostaining in rodent TBCs. In addition, immunostaining for GFP, which was expressed under the control of either the Ins1 or the Ins2 promoter in two separate mice strains, demonstrated that insulin is transcribed and translated in the TBCs of mice. We used ISH to demonstrate that insulin transcript is present only in the type II TBCs of the circumvallate, foliate, and fungiform papillae. We did not find insulin protein in the fungiform papillae; however, that could be due to insulin levels being lower than our threshold of detection. Transcription of the two rodent insulin genes was demonstrated by quantitative RT-PCR on mRNA extracts from both the posterior (containing the circumvallate and foliate papillae) and the anterior (containing the fungiform papillae) lingual epithelia. Similar to mouse islets of Langerhans, insulin 2 mRNA is the predominant form. Finally, we were able to measure immune-reactive insulin extracted from multiple pooled mouse lingual epithelia to verify translation and processing of the insulin gene.

Currently, the function of local insulin production in TBCs is unknown. On the basis of insulin's known functions, we can only speculate as to why insulin is produced in a subset of TBCs besides $\beta$ cells. Aside from regulating glucagon secretion from TBCs, it may be a trophic factor to TBCs, and it may be involved in differentiation decisions by the precursor cells. TBCs turn over rapidly, requiring a steady presence of growth factors to keep progenitor cells proliferating. The IGF family of peptides is an important regulator of growth and differentiation. Recently, it was demonstrated through use of a tongue-specific knockout of IGF receptor 1 that TBC growth is not dependent on IGF1 (45). Therefore, it is possible that insulin is a major growth factor driving TBC renewal. Because pancreatic insulin is unlikely to enter taste buds from the circulation because of their blood-bud barrier (46), local production of insulin was most likely retained throughout evolution for this purpose; we are currently testing this hypothesis.

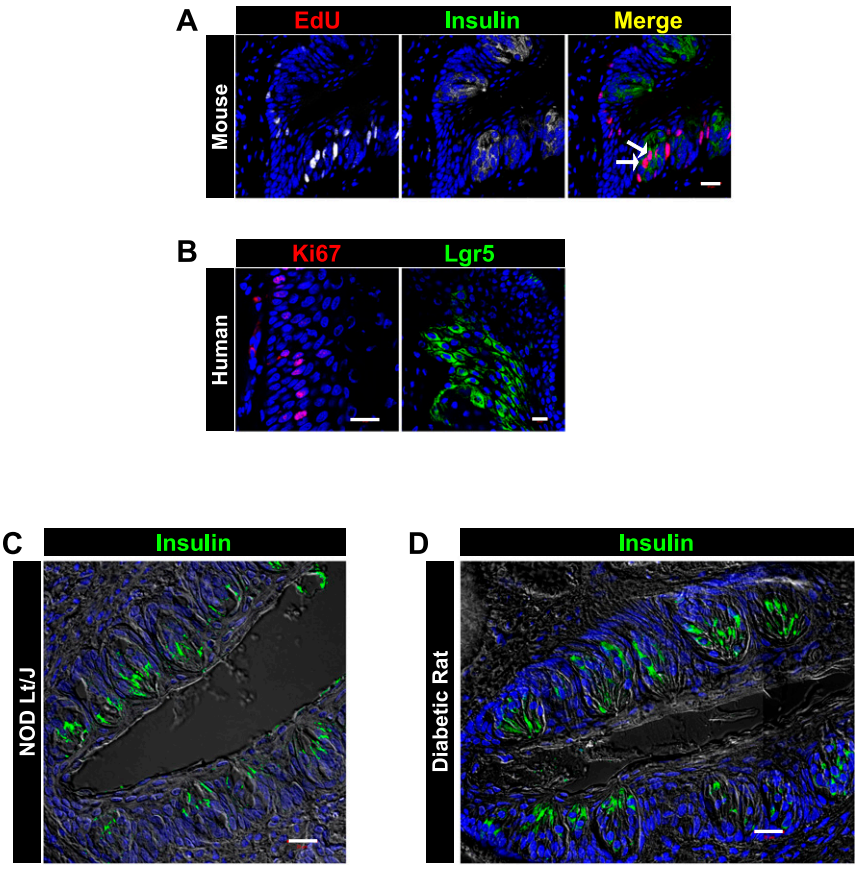


**Figure 6.** Insulin-positive taste cells are generated from highly proliferative progenitor cells in the tongue, and insulin is expressed in the TBCs of diabetic rodents. (A) EdU is detected in mature TBCs of C57BL6 mice that were injected with EdU 5 days before euthanasia. Note the presence of cells that exhibit chemical reactivity for EdU that are also immunoreactive for insulin (white arrows). Thus, perigemmal taste precursor cells had undergone proliferation in the previous 5 days and subsequently differentiated into mature TBCs that contained insulin. (B) Human lingual epithelium progenitor cells (Lgr5) also proliferated (Ki67) (male aged 76 years, human cadaveric tongue). Immunoreactive insulin is found in TBCs of two rodent models of diabetes namely the (C) NOD Lt/J (type 1 diabetes; blood glucose, 300 mg/dL) and (D) Sprague-Dawley rat (type 2 diabetes; blood glucose, 275 mg/dL). Scale bar, 20 μm.

It is also possible that lingual insulin has a direct functional role in taste perception similar to that of other hormones that are produced in both islets and TBCs. For example, glucagon and glucagonlike peptide-1 enhance sweet taste perception in TBCs (1). Because insulin expression in mouse TBCs appears to be confined to the type II TBCs, which detect sweet, umami, and bitter, it is possible that insulin acts to modulate perception of these tastants. Also, because insulin secretion from TBCs would be expected immediately upon glucose/fructose entering the TBCs, it may serve as the primary signal to inhibit lipolysis upon initiation of eating, thus perfectly coupling the arrival of an exogenous energy source with preservation of an internal energy source. Insulin is also known to induce vasodilation via nitric oxide–dependent pathways (47). Therefore, TBC-derived insulin may be involved in increasing blood flow to taste buds during eating, thereby increasing blood supply to progenitor cells and acting as a signal to differentiate and replace TBCs lost from mechanical injury. In addition, locally produced insulin likely enhances blood supply to von Ebner glands after eating. These glands secrete a lipase-containing serous fluid into the moats surrounding the circumvallate and foliate papillae that generates free fatty acids and flushes food residue from the moats and facilitates mastication (48).

## Conclusion

We have identified a highly proliferative cell population in the body—tongue epithelial cells—that expresses markers of endocrine progenitors and differentiates into insulin-synthesizing cells, namely TBCs, *in vivo*. A question now presents itself: Can these progenitor cells be expanded in culture conditions and differentiated into insulin-producing cells without the need for genetic reprogramming?

## Acknowledgments

*Financial Support:* This work was supported by NIA/NIH Grant 1ZIAAG000291-10 (to J.M.E.).

*Author Contributions:* M.E.D. designed the research, performed all the immunostaining and image acquisition for the images in the paper, and wrote the paper. J.L.F. assisted in all steps from initial conception through participation in the writing of the paper and oversaw animal handling and animal experiments. I.G.M. did the EdU experiment and the image processing for the immunostaining and participated in writing the paper. Q.-R.L. and E.G. did the RNAScope experiment. Q.-R.L. analyzed the quantitative RT-PCR experiment. E.G. isolated the lingual epithelium for quantitative RT-PCR and independently confirmed the insulin and taste cell marker colocalization experiments in the different rodent taste papillae. H.Y. and Y.-K.S. made the initial observations of the translation of insulin in the taste buds. S.S.-C.C. monitored the blood glucose of the NOD Shi/LtJ mice until they became diabetic and euthanized the mice for use in the immunostaining experiment. F.E.I. advised on the immunostaining, did image acquisition, and advised on the image processing. J.M.E. conceived the project and wrote the paper with M.E.D. J.M.E. is the guarantor of this work and, as such, had full access to all the data in the study and takes responsibility for the integrity of the data and the accuracy of the data analysis.

*Correspondence:* Josephine M. Egan, MD, National Institute on Aging, National Institutes of Health, 251 Bayview

Boulevard, Baltimore, Maryland 21224. E-mail: eganj@mail.nih.gov.

***Disclosure Summary:*** The authors have nothing to disclose.

## References


1. Calvo SS, Egan JM. The endocrinology of taste receptors. *Nat Rev Endocrinol*. 2015;**11**(4):213–227.
2. Kokrashvili Z, Yee KK, Ilegems E, Iwatsuki K, Li Y, Mosinger B, Margolskee RF. Endocrine taste cells. *Br J Nutr*. 2014;**111**(S1): S23–S29.
3. Shin YK, Martin B, Kim W, White CM, Ji S, Sun Y, Smith RG, Sévigny J, Tschöp MH, Maudsley S, Egan JM. Ghrelin is produced in taste cells and ghrelin receptor null mice show reduced taste responsivity to salty (NaCl) and sour (citric acid) tastants. *PLoS One*. 2010;**5**(9):e12729.
4. Newsholme P, Cruzat V, Arfuso F, Keane K. Nutrient regulation of insulin secretion and action. *J Endocrinol*. 2014;**221**(3): R105–R120.
5. Rorsman P, Braun M. Regulation of insulin secretion in human pancreatic islets. *Annu Rev Physiol*. 2013;**75**(1):155–179.
6. Feng P, Huang L, Wang H. Taste bud homeostasis in health, disease, and aging. *Chem Senses*. 2014;**39**(1):3–16.
7. Perea-Martinez I, Nagai T, Chaudhari N. Functional cell types in taste buds have distinct longevities. *PLoS One*. 2013;**8**(1):e53399.
8. Yee KK, Li Y, Redding KM, Iwatsuki K, Margolskee RF, Jiang P. Lgr5-EGFP marks taste bud stem/progenitor cells in posterior tongue. *Stem Cells*. 2013;**31**(5):992–1000.
9. Miura H, Scott JK, Harada S, Barlow LA. Sonic hedgehog-expressing basal cells are general post-mitotic precursors of functional taste receptor cells. *Dev Dyn*. 2014;**243**(10):1286–1297.
10. Ren W, Lewandowski BC, Watson J, Aihara E, Iwatsuki K, Bachmanov AA, Margolskee RF, Jiang P. Single Lgr5- or Lgr6-expressing taste stem/progenitor cells generate taste bud cells ex vivo. *Proc Natl Acad Sci USA*. 2014;**111**(46):16401–16406.
11. Gregg BE, Moore PC, Demozay D, Hall BA, Li M, Husain A, Wright AJ, Atkinson MA, Rhodes CJ. Formation of a human β-cell population within pancreatic islets is set early in life. *J Clin Endocrinol Metab*. 2012;**97**(9):3197–3206.
12. Yang H, Cong WN, Yoon JS, Egan JM. Vismodegib, an antagonist of hedgehog signaling, directly alters taste molecular signaling in taste buds. *Cancer Med*. 2015;**4**(2):245–252.
13. Hara M, Wang X, Kawamura T, Bindokas VP, Dizon RF, Alcoser SY, Magnuson MA, Bell GI. Transgenic mice with green fluorescent protein-labeled pancreatic beta -cells. *Am J Physiol Endocrinol Metab*. 2003;**284**(1):E177–E183.
14. Yong J, Rasooly J, Dang H, Lu Y, Middleton B, Zhang Z, Hon L, Namavari M, Stout DB, Atkinson MA, Tian J, Gambhir SS, Kaufman DL. Multimodality imaging of β-cells in mouse models of type 1 and 2 diabetes. *Diabetes*. 2011;**60**(5):1383–1392.
15. Gaillard D, Xu M, Liu F, Millar SE, Barlow LA. β-Catenin signaling biases multipotent lingual epithelial progenitors to differentiate and acquire specific taste cell fates. *PLoS Genet*. 2015; **11**(5):e1005208.
16. RRID:AB_10691857.
17. RRID:AB_726924.
18. RRID:AB_531826.
19. RRID:AB_942041.
20. RRID:AB_641123.
21. RRID:AB_260137.
22. RRID:AB_2126544.
23. RRID:AB_2142367.
24. RRID:AB_1310281.
25. RRID:AB_2314987.
26. RRID:AB_632197.
27. RRID:AB_261576.
28. RRID:AB_10563566.
29. RRID:AB_2535805.
30. RRID:AB_2534117.
31. RRID:AB_2534088.
32. RRID:AB_2338251.
33. RNAscope® Multiplex Fluorescent Reagent Kit v2 User Manual. Vol 323100-USM. Newark, CA: Advanced Cell Diagnostics Inc.; 2017.
34. Zhang HY, Bi GH, Li X, Li J, Qu H, Zhang SJ, Li CY, Onaivi ES, Gardner EL, Xi ZX, Liu QR. Species differences in cannabinoid receptor 2 and receptor responses to cocaine self-administration in mice and rats. *Neuropsychopharmacology*. 2015;**40**(4):1037–1051.
35. Luo X, Okubo T, Randell S, Hogan BL. Culture of endodermal stem/progenitor cells of the mouse tongue. *In Vitro Cell Dev Biol Anim*. 2009;**45**(1-2):44–54.
36. Doyle ME, Egan JM. Mechanisms of action of glucagon-like peptide 1 in the pancreas. *Pharmacol Ther*. 2007;**113**(3):546–593.
37. González-Mariscal I, Krzysik-Walker SM, Kim W, Rouse M, Egan JM. Blockade of cannabinoid 1 receptor improves GLP-1R mediated insulin secretion in mice. *Mol Cell Endocrinol*. 2016;**423**: 1–10.
38. Bartel DL, Sullivan SL, Lavoie EG, Sévigny J, Finger TE. Nucleoside triphosphate diphosphohydrolase-2 is the ecto-ATPase of type I cells in taste buds. *J Comp Neurol*. 2006;**497**(1):1–12.
39. Clapp TR, Yang R, Stoick CL, Kinnamon SC, Kinnamon JC. Morphologic characterization of rat taste receptor cells that express components of the phospholipase C signaling pathway. *J Comp Neurol*. 2004;**468**(3):311–321.
40. Yang R, Crowley HH, Rock ME, Kinnamon JC. Taste cells with synapses in rat circumvallate papillae display SNAP-25-like immunoreactivity. *J Comp Neurol*. 2000;**424**(2):205–215.
41. Soares MB, Schon E, Henderson A, Karathanasis SK, Cate R, Zeitlin S, Chirgwin J, Efstratiadis A. RNA-mediated gene duplication: the rat preproinsulin I gene is a functional retroposon. *Mol Cell Biol*. 1985;**5**(8):2090–2103.
42. Wentworth BM, Schaefer IM, Villa-Komaroff L, Chirgwin JM. Characterization of the two nonallelic genes encoding mouse preproinsulin. *J Mol Evol*. 1986;**23**(4):305–312.
43. Wang Y, Perfetti R, Greig NH, Holloway HW, DeOre KA, Montrose-Rafizadeh C, Elahi D, Egan JM. Glucagon-like peptide-1 can reverse the age-related decline in glucose tolerance in rats. *J Clin Invest*. 1997;**99**(12):2883–2889.
44. Rajagopal J, Anderson WJ, Kume S, Martinez OI, Melton DA. Insulin staining of ES cell progeny from insulin uptake. *Science*. 2003;**299**(5605):363.
45. Biggs BT, Tang T, Krimm RF. Insulin-like growth factors are expressed in the taste system, but do not maintain adult taste buds. *PLoS One*. 2016;**11**(2):e0148315.
46. Dando R, Pereira E, Kurian M, Barro-Soria R, Chaudhari N, Roper SD. A permeability barrier surrounds taste buds in lingual epithelia. *Am J Physiol Cell Physiol*. 2015;**308**(1):C21–C32.
47. Randriamboavonjy V, Schrader J, Busse R, Fleming I. Insulin induces the release of vasodilator compounds from platelets by a nitric oxide-G kinase-VAMP-3-dependent pathway. *J Exp Med*. 2004;**199**(3):347–356.
48. Voigt N, Stein J, Galindo MM, Dunkel A, Raguse JD, Meyerhof W, Hofmann T, Behrens M. The role of lipolysis in human orosensory fat perception. *J Lipid Res*. 2014;**55**(5):870–882.